AGU PUBLICATIONS

Geophysical Research Letters

RESEARCH LETTER
10.1002/2017GL074150

Key Points:
- The global ORCHIDEE ecosystem model is suitable for assimilating remotely sensed forest structure data to estimates AGB in tropical forests
- The FOTO-Pleiades products used for the assimilation system bear too large systematic errors to retrieve the fine-scale structure of AGB
- Most of the systematic errors related to ORCHIDEE-CAN could be reduced by improving the allometric equations

Supporting Information:
- Supporting Information S1

Correspondence to:
E. Joetzjer,
emilie.joetzjer@lsce.ipsl.fr

Citation:
Joetzjer, E. et al (2017), Assimilating satellite-based canopy height within an ecosystem model to estimate aboveground forest biomass, *Geophys. Res. Lett.*, *44*, doi:10.1002/2017GL074150.

Received 14 MAY 2017
Accepted 27 JUN 2017
Accepted article online 5 JUL 2017

Assimilating satellite-based canopy height within an ecosystem model to estimate aboveground forest biomass

E. Joetzjer[1,2,5], M. Pillet[1,3], P. Ciais[2], N. Barbier[4], J. Chave[5], M. Schlund[6], F. Maignan[2], J. Barichivich[7,8], S. Luyssaert[9], B. Hérault[10], F. von Poncet[11], and B. Poulter[1,12]

[1]Department of Ecology, Montana State University, Bozeman, Montana, USA, [2]Laboratoire des Sciences du Climat et de l'Environnement, LSCE-IPSL (CEA-CNRS-UVSQ), Gif-sur-Yvette, France, [3]Department of Ecology and Evolutionary Biology, University of Arizona, Tucson, Arizona, USA, [4]IRD UMR AMAP, Botany and Modeling of Architecture of Plants and Vegetations, Montpellier, France, [5]Laboratoire Evolution et Diversité Biologique, Toulouse, France, [6]European Space Research and Technology Centre, European Space Agency, Nordwijk, Netherlands, [7]Instituto de Conservación, Biodiversidad y Territorio, Universidad Austral de Chile, Valdivia, Chile, [8]Center for Climate and Resilience Research, Santiago, Chile, [9]Department of Ecological Sciences, Vrije Universiteit (VU), Amsterdam, Netherlands, [10]CIRAD, UMR Ecologie des Forêt de Guyane, Kourou, France, [11]Airbus Defence and Space, ImmenstaadGermany, [12]Biospheric Sciences Laboratory, NASA Goddard Space Flight Center, Greenbelt, Maryland, USA

Abstract Despite advances in Earth observation and modeling, estimating tropical biomass remains a challenge. Recent work suggests that integrating satellite measurements of canopy height within ecosystem models is a promising approach to infer biomass. We tested the feasibility of this approach to retrieve aboveground biomass (AGB) at three tropical forest sites by assimilating remotely sensed canopy height derived from a texture analysis algorithm applied to the high-resolution Pleiades imager in the Organizing Carbon and Hydrology in Dynamic Ecosystems Canopy (ORCHIDEE-CAN) ecosystem model. While mean AGB could be estimated within 10% of AGB derived from census data in average across sites, canopy height derived from Pleiades product was spatially too smooth, thus unable to accurately resolve large height (and biomass) variations within the site considered. The error budget was evaluated in details, and systematic errors related to the ORCHIDEE-CAN structure contribute as a secondary source of error and could be overcome by using improved allometric equations.

1. Introduction

Tropical deforestation and forest degradation are major contributors of annual CO_2 emissions to the atmosphere [*Ciais et al.,* 2014; *Pütz et al.,* 2014]. Considering the different carbon flux components of net deforestation emissions separately [*Richter and Houghton*, 2011], gross deforestation releases approximately 4.3 Pg C yr^{-1}, while secondary forest regrowth absorbs 2.8 Pg C yr^{-1}, resulting in net land use change emissions of 1.5 Pg C yr^{-1} [*Houghton*, 2013; *Le Quéré et al.,* 2015]. At present, deforestation emissions mostly occur in the tropics and represent about 1 Pg C yr^{-1} [*Baccini et al.,* 2012]. However, the uncertainty surrounding these estimates remains substantial (0.5 Pg C yr^{-1} [*Houghton et al.,* 2012]). Part of the uncertainty in tropical land use and land-cover change (LULCC) emissions is associated with mapping deforestation and degradation areas, but recent high-resolution satellite observations offer the possibility to significantly reduce this source of uncertainty [*Hansen et al.,* 2013; *Mitchard et al.,* 2014]. A second important source of uncertainty is from poorly known initial biomass carbon stocks and delayed soil emissions consecutive to LULCC disturbances [*Hurtt et al.,* 2004].

At present, the best approaches to estimate biomass are labor-intensive forest inventories. At stand level, forest canopy height is commonly related to biomass using empirical allometric equations derived from field surveys [*Saatchi et al.,* 2011; *Asner et al.,* 2012]. For example, the Lorey's height defined by the height of a stand weighted by the basal area for all trees >10 cm diameter explains a high degree of variance in stand level biomass, with a root-mean-square error of around 25% [*Saatchi et al.,* 2011]. Contemporary spaceborne light detection and ranging (lidar) remote sensing can now measure the height of the largest trees and have been used to estimate aboveground biomass (AGB) at landscape scales, by converting canopy height using empirical relationships [*Vincent et al.,* 2012; *Réjou-Méchain et al.,* 2015]. Pantropical AGB maps have been produced using spaceborne lidar remote sensing, but they strongly differ among each other [*Saatchi et al.,* 2011; *Baccini et al.,* 2012].

Spaceborne radar data offer another alternative to map biomass due to their varying penetration capabilities [*Shimada et al.,* 2010], and the backscattering signal has been shown to correlate with AGB [*Toan et al.,* 2011]. In general, this correlation tends, however, to saturate at high biomass (around 150 t/ha) in the L-band [*Mermoz et al.,* 2015] and at higher values in P-band [*Dubois-Fernandez et al.,* 2012]. The phase information of an interferometric synthetic aperture radar (SAR) system is more sensitive compared to backscatter and could overcome the saturation limit [*Schlund et al.,* 2015]. X-band radar data have a finer spatial resolution than L- or P-band data, allowing the identification of individual tree crowns or small forest patches [*Ho Tong Minh et al.,* 2016]. TanDEM-X is a SAR mission acquiring interferometric data via an across-track configuration minimizing temporal decorrelation [*Krieger et al.,* 2007]. The interferometric coherence at X-band, although not a direct measure of AGB, was found to be moderately correlated with AGB ($R^2 \approx 0.5$) [*Schlund et al.,* 2015]. TanDEM-X data were acquired consistently several times and processed over the entire landmass [*Krieger et al.,* 2007], but the original data have not yet been made available over large regions to study vegetation structure.

High-resolution optical imagers (with a resolution of less than 1 m) also have the potential to characterize individual tree forms in tropical canopies and thus to inform on forest structure and (indirectly) on biomass, considering the fact that AGB and forest height are mostly driven by the largest trees that can be seen by optical imagers [*Slik et al.,* 2013; *Bastin et al.,* 2015]. It is this potential that is investigated in this study. The Fourier Transform Textural Ordination (FOTO) method was developed more than a decade ago for tropical forests [*Couteron et al.,* 2005], with the objective to derive canopy textural properties into a few informative features. The approach has now been applied to a number of sites across the tropics, and statistical relationships between texture features and forest structural parameters as measured in 1 ha field plots often showed remarkably good R^2 values (above 0.8) and RMSE below 15% [*Proisy et al.,* 2007; *Barbier et al.,* 2010; *Ploton et al.,* 2012; *Bastin et al.,* 2014] but varied substantially from site to site [*Ploton et al.,* 2013] due to changes in forest structure, gap distribution, variations in diameter at breast height (DBH)-height relationships, vertical structure, and topography [*Bastin et al.,* 2014]. Texture-height relationships have been little explored (but see *Couteron et al.* [2005]) but are expected to exist given the relationship between crown size distribution as assessed by the FOTO method, and height distribution, or more generally, crown size and height or DBH [*Blanchard et al.,* 2016].

Irrespective of the remote sensing technology, height-biomass relationships are required and the derivation, for example, of a Lorey's height-biomass relationship in the field is labor intensive and site specific. Alternatively, we hypothesize in this study that a process-based model of vegetation could be used to simulate the relationship between height and biomass as this model includes processes contributing to the stand dynamics, especially crowding competition processes, often described by self-thinning laws. The advantage of a process-based model is that it can be calibrated at few locations, and its results extrapolated over larger spatial scales where no allometric data are available. Height observations can then be converted into AGB by applying the simulated height-biomass relationships.

Here we describe a new assimilation framework of canopy height into AGB, based on assimilation principles previously applied using pseudodata in temperate forests [*Bellassen et al.*, 2011] and airborne lidar height in Costa Rica [*Hurtt et al.,* 2010], using the Organizing Carbon and Hydrology in Dynamic Ecosystems Canopy (ORCHIDEE-CAN) process-based ecosystem model which includes stand dynamics equations and crowding competition between individuals [*Naudts et al.,* 2015]. The feasibility of this method is tested for mapping AGB at three contrasted tropical forests located in French Guiana and Cameroon. Because future satellite missions are planned to provide global coverage using next generation spaceborne lidar measurements [*Morton*, 2016], and P-band radar [*Ho Tong Minh et al.,* 2014], it is therefore urgent to assess how this information will be assimilated in ecosystem models to improve AGB monitoring.

2. Methods

A flowchart describing the assimilation of the Pleiades-FOTO-derived tree height into ORCHIDEE-CAN ecosystem model and the benchmarking processes against census and TanDEM-X data is given in the supporting information (Figure S1).

2.1. Study Sites and Forest Census Data

Three old-growth tropical rain forest sites are used in this study. The forests of Paracou (5.18°N, 52.55°W) and Nouragues Ecological Research Stations (4.05°N, 52.4°W) are located in French Guiana, South America. They both have a humid climate (3000 mm yr^{-1}) with a 2 month dry season (< 100 mm) from late August to early November. Nouragues forests are on a clayey soil, hilly terrain with the presence of a granitic outcrop, and approximately 200 tree species per hectare. Paracou is on sandy-clayey soil, with a more regular topography and approximately 150 tree species per hectare. The third site is the forest of Pallisco (3.38°N, 13.66°E) in Eastern Cameroon. It has a drier climate (1739 mm yr^{-1}), a longer dry season from November to February, and has undergone selective logging in the recent past.

Nouragues has two large permanent inventory plots: Grand Plateau (1000 × 100 m) and Petit Plateau (400 × 300 m) subdivided into 22 subplots of 100 × 100 m in total. Paracou has seven inventory plots, regularly measured since 1984, with six plots of 250 × 250 m and one of 500 × 500 m [*Ho Tong Minh et al.,* 2016]. In Cameroon, besides the Pallisco FMU10041 concession, data from Lomie (3.070°N, 13.58°E) and DengDeng (5.22°N, 13.40°E) have also been used to increase the number of available observations and reach fifty 1 ha plots where repeated inventories have been collected from 2006 to 2014. We used inventories made in 2012, 2014, and 2011 at respectively Nouragues, Paracou, and Cameroon to match as much as possible Pleiades acquisition.

AGB was calculated for each tree as follows [*Chave et al.,* 2014]:

$$\mathrm{AGB} = 0.0673\ \left(\rho\ d^2\ H\right)^{0.976} \tag{1}$$

where H is tree height (m), d is the trunk diameter at breast height (DBH; cm), and ρ is the oven-dry wood density (g/cm^3). In French Guiana, tree heights were not directly measured but inferred from DBH (cm) using the following generic equation [*Chave et al.,* 2014]:

$$H = \exp\left[0.893 - E + 0.760\ \ln(d) - 0.0340\ [\ln(d)]^2\right] \tag{2}$$

Here E represents a metric of environmental stress which, for a given diameter, decreases the value of tree height with water and temperature stress (see supporting information) [*Chave et al.,* 2014, equation (6b)]. In Cameroon, tree height was directly measured over a subsample of trees ($N > 50$ trees) in each plot to calibrate a local DBH-height allometric equation applied to deduce the height of the remaining trees in the plot. Then, AGB for this site was derived using equation (1).

Wood density values were extracted from the Global Wood Density Database [*Chave et al.*, 2009, www.datadryad.org]. When multiple wood density measurements for one species were available, the median was used. For trees not identified to species, genus or family medians were used. For families not represented in the database, the median density for tropical South America was used. Estimated tree level AGB values were summed over each plot to yield a stand level total that was then used to evaluate AGB estimates from assimilating remote sensing data in the ORCHIDEE-CAN model.

2.2. Estimating Forest Height Using Textural Analysis of the Pleiades Optical Imager

Considering the dominance of larger trees in tropical forest dynamics and in stand level AGB [*Stephenson et al.,* 2014; *Fauset et al.,* 2015], the 95th canopy height percentile (H_{95}) is chosen as the target variable that will be assimilated. To extrapolate heights at the landscape level, we used textural features extracted from the panchromatic band of Pleiades images at 0.5 m resolution, using the FOTO method [*Couteron et al.*, 2005; *Barbier and Couteron*, 2015]. In short, the images were subdivided into 100 m long subwindows that were used to characterize local textural properties of the canopy. In order to improve the detection of limits between forest types and the spatial correspondence with ground data, a sliding window approach was used to extract these windows every 25 m. Each image extract was then converted to a 2-D power spectrum via 2-D fast Fourier transform and the subsequent computation of squared amplitudes, thus discarding all phase information. A second step of simplification consisted in averaging power spectra across directions, to conserve only spatial frequency-related information. The resulting table of radial spectra was further simplified thanks to a principal component analysis (PCA), aiming at identifying the two or three main axes of textural variation in the satellite image,

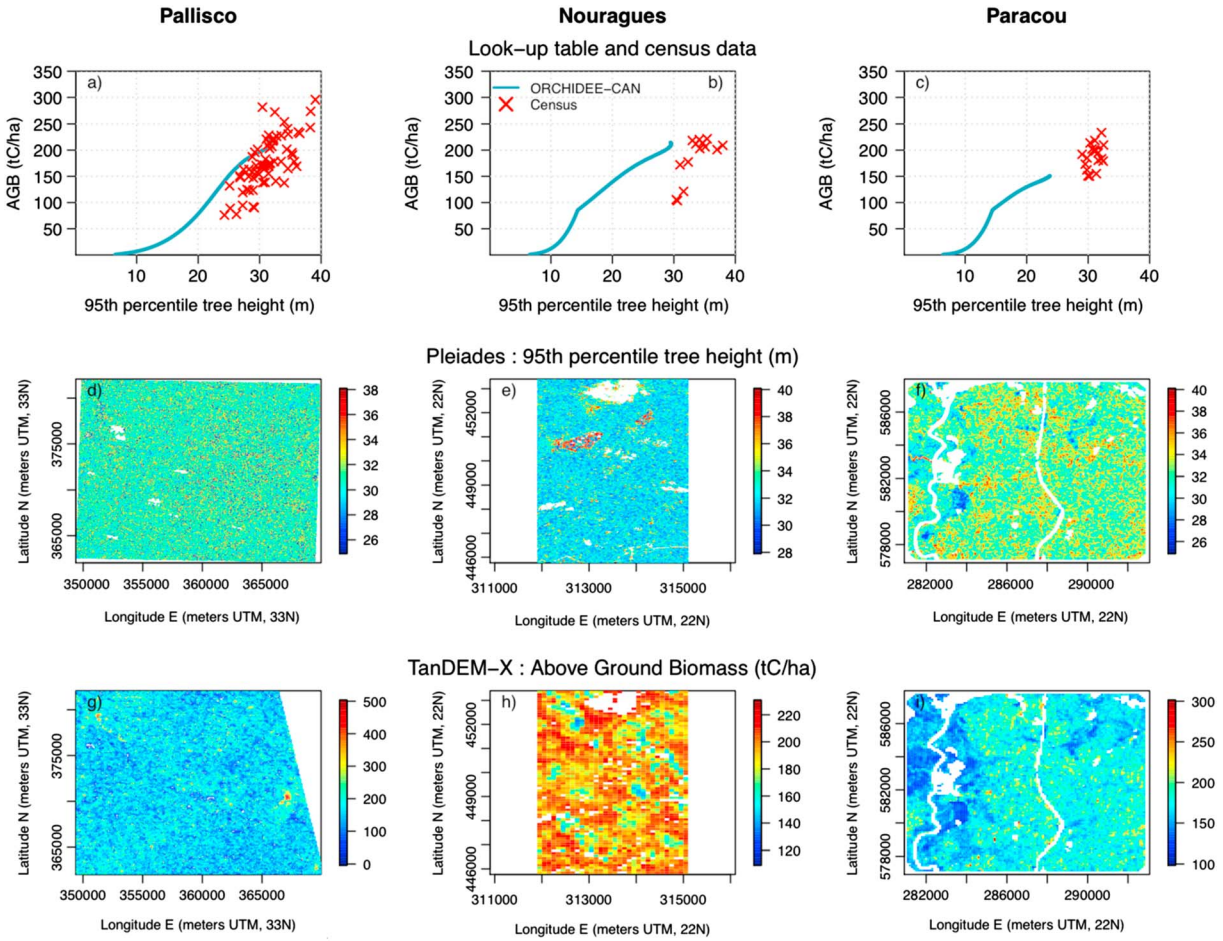

Figure 1. For the three studied sites are represented, (a–c) AGB (t C ha^{-1}) versus 95th percentile canopy height simulated by ORCHIDEE-CAN over 400 years and from the inventory data as well as the (d–f) 95th percentile canopy height (m) from Pleiades at a resolution of 25 m × 25 m and the (g–i) AGB from TanDEM-X at of resolution of 100 m × 100 m. Rivers (at Paracou) and hilly areas (at Nouragues) were masked using lidar data.

generally corresponding to gradients of coarseness-fineness and heterogeneity in the canopy images. The approach is therefore analogous to a Gabor filter or a windowed/local Fourier transform, coupled with a PCA analysis.

The first three principal components were then used to estimate canopy height using a multiple linear regression model calibrated using canopy heights estimated in the field plots, using the closest inventory year to the remote sensing data year. The linear regression model has an R^2 of 0.56, 0.43, and 0.52 for Cameroon, Nouragues, and Paracou, respectively (Figure S2). Although this is comparable with previous efforts (e.g., R^2 = 0.57 in *Couteron et al.* [2005]), this relatively low correlation is clearly a limitation of our approach to assimilate height into AGB. The resulting height model was then used to predict the H_{95} over the entire area covered by each Pleiades scene (Figures 1d–1f) and was evaluated against airborne lidar canopy height observations at 1 m resolution [*Vincent et al.,* 2012] available only at the French Guiana sites (section 3.3.3). Lidar uses emitted laser pulses to measure the distance from the sensor to the surfaces in its path and has been used mainly to extract canopy heights.

2.3. ORCHIDEE-CAN: Simulations and Assimilation Approach

The model used for assimilating H_{95} into AGB is ORCHIDEE (Organizing Carbon and Hydrology in Dynamic Ecosystems), a process-based ecosystem model first described in *Krinner et al.* [2005] which mechanistically represents energy, water, and carbon exchanges within the soil-plant-atmosphere continuum using a "big-leaf" approach. The ORCHIDEE-CAN version [*Naudts et al.*, 2015] drops the big-leaf approach and simulates forest structure, with stand dynamics processes including recruitment and

demography represented by downscaling stand level net primary productivity (NPP) to 20 cohorts following the allocation rules of *Deleuze et al.* [2004], as originally implemented by *Bellassen et al.* [2010]. Mortality due to competition between cohorts is based on the self-thinning equation [*Reineke*, 1933], which is usually verified in temperate and boreal stands, and was also proven valid, albeit with a larger noise, in tropical forests [*Kohyama*, 1992; *Phillips et al.*, 2002]. The version of ORCHIDEE-CAN used in this study does not include climate-induced mortality and has no specific gap formation equation since individual tree gaps are implicitly included in the self-thinning mortality formulation. ORCHIDEE-CAN was originally developed and calibrated for European forests. Thus, in this study, we have recalibrated allometric, physiological, and demographic parameters using specific observations for the Amazonian tropical forests [*Asner et al.*, 2002; *Kattge et al.*, 2011; *Goodman et al.*, 2014] (see supporting information) corresponding to the tropical rain forest evergreen plant functional type (PFT) in the model (Tables S1a and S1b).

ORCHIDEE-CAN was run over a single grid cell at each of the three forest sites using as input the gridded climate forcing data from CRUNCEP, which combines monthly data from the Climate Research Unit (CRU) and 6-hourly variations from the National Center for Environmental Prediction (NCEP) [*Wei et al.,* 2014]. The 0.5° grid cell of CRUNCEP corresponding to each site was selected to force the model, without any further downscaling. A semianalytical spin-up [*Lardy et al.,* 2011] was performed using the climate data from 1901 to 1930 to equilibrate carbon and hydrological state variables. Following the spin-up, and after removing all living biomass, ORCHIDEE-CAN was run for 400 years by cycling through the climate data from 1971 to 2000 under a CO_2 concentration set at 346 ppm to represent the average current growing conditions.

ORCHIDEE-CAN simulates for each site a statistical distribution of tree heights across its 20 cohorts, from which H_{95} was calculated, as well as the simulated relationship between H_{95} and AGB (Figures 1a–1c). We sampled the satellite-based observations of H_{95} from the FOTO Pleiades analysis for each grid cell of 25 m (see section 2.2 and data in Figures 1d–1f) and matched its value with the most similar H_{95} simulated by ORCHIDEE-CAN. The corresponding AGB estimates were then extracted as being the AGB modeled by ORCHIDEE-CAN that corresponds with the matched ORCHIDEE-CAN H_{95} for every grid cell in the FOTO-Pleiades product.

2.4. Benchmarking of Assimilated AGB Against Census Data

AGB values assimilated against H_{95} from FOTO-Pleiades were compared against census data rasterized at 1 ha resolution. Edge cells were removed to avoid evaluating assimilated AGB in grid cells with incomplete inventory data.

2.5. Independent Comparison Against AGB From X-Band Radar

In addition to census data, we also compared assimilated AGB with AGB retrieved from X-band radar remote sensing data from the TerraSAR-X add-on for Digital Elevation Measurement (TanDEM-X) mission (Figures 1g–1i). TanDEM-X is a high-resolution interferometric SAR mission using two satellites (TanDEM-X and TerraSAR-X) in bistatic mode (see supporting information) [*Bamler and Hartl*, 1998; *Kugler et al.,* 2014; *Schlund et al.,* 2015]. AGB from TanDEM-X was evaluated against AGB derived from the census data to evaluate its quality (supporting information Table S2), RMSE varies from 24 t C ha^{-1} (13%) to 49 t C ha^{-1} (27%) suggesting a moderate (but still useful) ability of TanDEM-X AGB to reproduce mean AGB values across the three tropical forests studied here. Therefore, the comparison between assimilated AGB with AGB derived from TanDEM-X is considered as informative only, because the spatial accuracy of AGB from X-band radar has never been estimated for the three sites of this study. While AGB from TanDEM-X is not as accurate as the ones from census data, it allows to better define the statistics of the spatial error distribution of AGB obtained by assimilating FOTO-Pleiades H_{95} with ORCHIDEE-CAN. AGB from TanDEM-X was rasterized to 1, 4, and 9 ha to calculate the scale dependency of errors.

2.6. Decomposition of the Uncertainties of Assimilated AGB

Uncertainties, i.e., the differences between assimilated and pseudo-observed AGB, were decomposed using the approach from *Kobayashi and Salam* [2000]. In this approach, the total uncertainty, the mean square

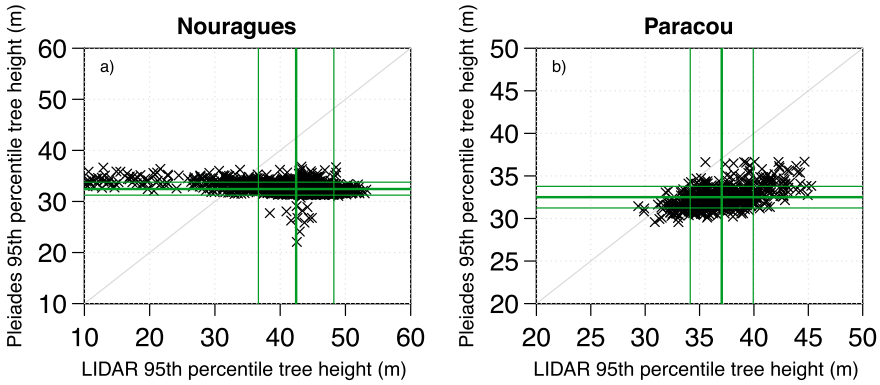

Figure 2. Scatterplot of the 95th percentile canopy height derived from Pleiades versus 95th percentile derived from lidar gridded at 100 m × 100 m at (a) Nouragues and (b) Paracou. Green lines represent the mean and deviation of each product.

deviation ($MSD = RMSE^2$) of modeled AGB compared to the observations, is decomposed into three additive components:

$$MSD = SB + SDSD + LCS \tag{3}$$

SB (equation (4)) represents the squared bias of AGB simulated by ORCHIDEE/Pleiades (x) from the AGB derived from TanDEM-X (y), as we could not use census data as observed because there were not enough measured plots. So we use Tandem-X AGB instead, keeping in mind some of its limitations (e.g., the Sinnamary River in Figure 1i at the Paracou forest, where Tandem-X AGB is too low).

$$SB = (\overline{x} - \overline{y})^2 \tag{4}$$

SDSD (equation (5)) is the squared difference between standard deviations (i.e., the difference in the magnitude of spatial variance between the simulation and measurement).

$$SDSD = \left(SD_x - SD_y\right)^2 \tag{5}$$

where SD_x and SD_y are the standard deviations of the AGB simulated by ORCHIDEE/Pleiades and derived from TanDEM-X, respectively. LCS (lack of correlation weighted by the standard deviations; equation (6)) describes the spatial coherence between observed and modeled fields.

$$LCS = 2SD_x SD_y\,(1 - r) \tag{6}$$

With r the correlation coefficient calculated as follows:

$$r = \left[\frac{1}{n}\sum_{i=1}^{n}(x_i - \overline{x})(y_i - \overline{y})\right] / \, SD_x SD_y \tag{7}$$

3. Results and Discussion

3.1. Canopy Heights From FOTO-Pleiades Compared to Airborne Lidar Canopy Height Observations

When compared to independent and more accurate airborne lidar mean canopy height observations, the FOTO-Pleiades product underestimates H_{95} on average by 10 m at Nouragues and by 3 m at Paracou and poorly captures the spatial variability of canopy heights (Figure 2), especially at Nouragues, likely because of a hilly topography. This excessively homogeneous distribution of height in FOTO-Pleiades will thus result in a lack of fine scale structure after the assimilation of H_{95} in ORCHIDEE-CAN.

3.2. AGB From the Assimilation of FOTO-Pleiades 95th Percentile Height

The ORCHIDEE-CAN simulated relationship between AGB and H_{95} height performs well compared to census data (Figures 1a–1c) at Pallisco (Figure 1a) but underestimates H_{95} (about 4 m) and yet slightly overestimates AGB (about 30 t C ha^{-1}) at Nouragues (Figure 1b) and underestimates both H_{95} (about 7 m) and AGB (about 40 t C ha^{-1}) at Paracou (Figure 1c). Even though ORCHIDEE-CAN has been calibrated using tropical forest measurements, it describes all tropical forests using the same parameters of the evergreen broadleaved forest PFT, the same NPP increment allocation rules [*Deleuze et al.,* 2004] and self-thinning mortality equation [*Reineke*, 1933]. This induces some constraints in the model, explaining local differences in the H_{95}-AGB relationship across the three forest sites studied.

First, we compared assimilated and census-observed mean AGB. Assimilating H_{95} from FOTO-Pleiades (see Figure 1) to infer AGB provides mean values of 189, 210, and 157 t C ha^{-1} at Pallisco, Nouragues, and Paracou, respectively. These mean values are obtained from the average of the assimilated AGB distribution aggregated at 1 ha resolution (section 2.3). As a comparison, the mean AGB estimated from census data (section 2.1) is at 181, 188, and 185 t C ha^{-1} at Pallisco, Nouragues, and Paracou, respectively. AGB from the global data sets from *Baccini et al.* [2012] and *Saatchi et al.* [2011] are lower than both census data and our assimilated AGB results, with *Saatchi et al.* [2011] [*Baccini et al.*, 2012] providing AGB of 162 (169), 142 (140), and 117 (133) t C ha^{-1} at Pallisco, Nouragues, and Paracou, respectively.

Second, comparing the spatial distribution of assimilated and census-based AGB, rasterized at 1 ha resolution gives RMSE of 62 (34%), 49 (26%), and 53 (30%) t C ha^{-1} at Pallisco, Nouragues, and Paracou, respectively. Despite these reasonable performances at first glance, the assimilated AGB distribution is extremely homogeneous (reflecting the one of FOTO-Pleiades) compared to the census data, which is a clear limitation of our results.

While census data are the most reliable benchmark data, they do not cover a large enough area, only with 68, 14, and 18 1 ha plots being available, to derive a robust characterization of the error budget of assimilated AGB. Therefore, the assimilated AGB errors were analyzed against TanDEM-X-AGB at 1 ha resolution for each site. The RMSE of assimilated AGB versus TanDEM-X is of 68 (42%), 25 (13%), and 29 (15%) t C ha^{-1} at Pallisco, Nouragues, and Paracou. These figures are comparable with the performances of AGB models based on remote sensing data from 23 studies across the globe [*Mitchard*, 2015, Table 1], with RMSE ranging from 19 to 53% depending on the method used. Thus, our approach based on FOTO-Pleiades is in the range of the current remote sensing methods, but still insufficient to characterize AGB with an accuracy comparable to census-based or airborne lidar.

3.3. Error Analysis

3.3.1. Error Related to the Structure of ORCHIDEE-CAN

Across the three sites, the ORCHIDEE-CAN assimilation appears to perform better for AGB at the French Guiana sites than at Pallisco. Assimilated AGB is overestimated at Pallisco and Nouragues and underestimated at Paracou (Figures 3c–3e). The square bias (SB) is lower at the French Guiana sites (Figures 3a–3c) partly because of lower structural errors in ORCHIDEE-CAN that was calibrated using observation from the Amazon forest. Further, the climate forcing data from CRUNCEP are a substantial source of uncertainty, especially at tropical locations where spatial precipitation variability is not well captured by the interpolation of CRU stations data, and temporal variability not well reproduced by NCEP. Our cross-site comparison argues for site-specific model calibration, or at least improving representation of tropical forest plant diversity representation [*van Bodegom et al.,* 2014], as well as the use of long-term local meteorological drivers, in order to reduce uncertainty in AGB estimation.

3.3.2. Errors Related to the Assimilation Method

The assimilation method itself also bears uncertainty, in particular, the H_{95} chosen as a target variable for the assimilation is only one measure of forest structure and was selected as a least biased estimator. But the sensitivity of AGB to the choice of assimilating mean height, median height, or maximum height can be more quantitatively addressed. Neighborhood size is generally very sensitive to scale (i.e., assimilation errors are scale dependent), for example, when ORCHIDEE/Pleiades-derived AGB is aggregated at 1, 4, and 9 ha and compared against TanDEM-X, the overall error decrease with coarser resolution. While SBs slightly decreases, MSD decreases are mostly explain by decreases of the SDSDs (equation (5); Figures 3a–3c), meaning that

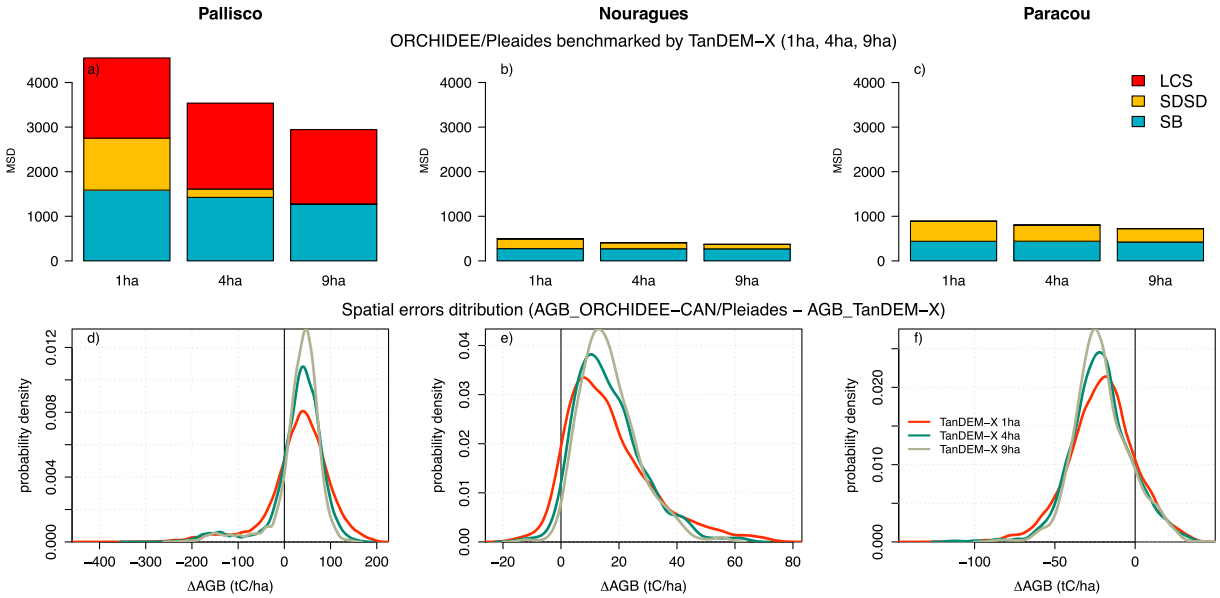

Figure 3. For the three sites, (a–c) benchmarking results of the AGB estimated by ORCHIDEE-CAN/Pleiades against TanDEM-X aggregated at 1, 4, and 9 ha using the mean square deviation (MSD) decomposition into SB (standard bias), SDSD (squared difference between standard deviations), and LCS (lack of correlation weighted by the standard deviations) and (d–f) probability density functions of the spatial distribution of the errors in t C ha^{-1} ($AGB_{ORCHIDEE\text{-}CAN/Pleiades} - AGB_{TanDEM\text{-}X}$).

ORCHIDEE-CAN/Pleiades AGB better captures the magnitude of variability of AGB derived from TanDEM-X at coarser spatial resolution. This illustrates that errors in initialization tend to be compensated at larger spatial scales, as shown by *Hurtt et al.* [2010].

3.3.3. Errors Related to Forest Structure Data

Comparing canopy heights from FOTO-Pleiades to airborne lidar measurements shows the poor ability of this height product to correctly capture the high spatial variability of canopy height, inability which can increase by site-specific characteristics as illustrated at Nouragues (Figure 2). This explains the low MSDs at Nouragues and Paracou because of LCS being close to 0 in Figures 3b and 3c. Besides, census data are used to calibrate remote sensing (FOTO or interferometric coherence) algorithm and infer forest structure variables, except at Pallisco where enough data were available to independently use a calibration and evaluation sample. To overcome this, more ground data are needed to independently derive forest structure variables (H_{95} or AGB) from remote sensing when benchmarking is also performed against census data.

Additionally, the quality of AGB and canopy height estimates from inventory data is sensitive to the specific form of the allometric equations used to estimate these variables, and the values of the parameters in these relationships. While errors can be large at tree level, they tend to average out when considering a population of trees, with, for example, a 90% accuracy in AGB stock estimation at 0.25 ha scale [*Chave et al.,* 2014].

4. Conclusions

Biomass estimates across the tropics remain highly uncertain [*Mitchard et al.,* 2014]. Here we estimated AGB at three tropical forest sites by assimilating the H_{95} inferred from remote sensing images processed with a texture analysis algorithm into height distributions into the ORCHIDEE-CAN large-scale ecosystem model. Overall, by making use of the FOTO-Pleiades data, the proposed method estimates the mean AGB within 10% of the census observation, with 4, 12, and 15% errors at Pallisco, Nouragues, and Paracou, respectively. Although this result may look encouraging compared to the accuracy of published remote sensing-based estimates of AGB, it masks a poor ability of our assimilation method to retrieve the small-scale variability of AGB, because the FOTO-Pleiades height is too homogeneous. Therefore, our results are still insufficiently accurate to characterize AGB within the accuracy of census-based observations or airborne lidar retrievals. However, a DGVM-type ecosystem model designed for large-scale applications like ORCHIDEE-CAN was here shown conceptually suitable for assimilating remotely sensed forest structure data to estimates AGB in

tropical forests, because this model includes a simulation of competition processes. Although DGVM models will likely remain less accurate locally than a detailed stand growth model calibrated for a specific site, our result points out to technical feasibility to assimilate large-scale satellite information with this type of models in the future.

There are several ways to improve the method described here as a feasibility test. First, the model could be optimized (calibrated) using site-specific physiological and ecological data and forced with observed instead of large scale analyzed climate forcing. Second, the FOTO-Pleiades products should certainly be improved to better reconstruct heights distributions, using, e.g., topographic information. Last, using the same assimilation framework, other height products could be assimilated into AGB. In particular, assimilating airborne lidar data or global-scale existing forest canopy height data sets [e.g., *Lefsky*, 2010] into AGB could be attempted to further demonstrate the potential of the proposed method. The diversity of algorithms used to interpret remote sensing data will continue to improve in the future, especially in terms of capturing spatial variability from forest degradation or small-scale disturbances. Integrating ecosystem models with a new generation of data from the European Space Agency Biomass Mission [*Le Toan et al*., 2011] or the NASA GEDI Mission [*Stysley et al.,* 2015] will help in providing improved estimates of global biomass, as well as other ecosystem variables.

Acknowledgments
The authors are grateful to Philippe Peylin for helpful discussions and to Victoria Meyer and Sassan Saatchi for providing lidar data and acknowledge the Gordon and Betty Moore Foundation NERC Consortium Grants "AMAZONICA" (NE/F005806/1), the "Investissement d'Avenir" grants managed by Agence Nationale de la Recherche (CEBA, ref. ANR-10-LABX-25-01; TULIP: ANR-10-LABX-0041; ANAEE-France: ANR-11-INBS-0001), and the European Union Climate KIC grant FOREST Specific Grant Agreement EIT/CLIMATE KIC/SGA2016/1CNES (TOSCA program) for funding. P.C. received support from the European Research Council Synergy grant ERC-2013-SyG-610028 IMBALANCE. P.J.B. received funding from $(CR)^2$ Chile (CONICYT/FONDAP/15110009). To access the remote sensing data, please contact Nicolas Barbier (nicolas.barbier@ird.fr) for Pleiades, Felicitas von Poncet (felicitas.poncet@airbus.com) for TanDEM-X, and Jerôme Chave (jerome.chave@univ-tlse3.fr) for lidar. We thank Bayani Cardenas, Martin Thurner, and one anonymous reviewer for critical reviews of the manuscript. The authors dedicate this paper to our colleague and dear friend Nicolas Najdovski.

References

Asner, G. P., M. Palace, M. Keller, R. Pereira, J. N. M. Silva, and J. C. Zweede (2002), Estimating canopy structure in an Amazon Forest from laser range finder and IKONOS satellite observations, *Biotropica*, *34*(4), 483–492, doi:10.1646/0006-3606(2002)034[0483:ECSIAA]2.0.CO;2.

Asner, G. P., J. Mascaro, H. C. Muller-Landau, G. Vieilledent, R. Vaudry, M. Rasamoelina, J. S. Hall, and M. van Breugel (2012), A universal airborne LiDAR approach for tropical forest carbon mapping, *Oecologia*, *168*(4), 1147–1160, doi:10.1007/s00442-011-2165-z.

Baccini, A., et al. (2012), Estimated carbon dioxide emissions from tropical deforestation improved by carbon-density maps, *Nat. Clim. Change*, *2*(3), 182–185, doi:10.1038/nclimate1354.

Bamler, R., and P. Hartl (1998), Synthetic aperture radar interferometry, *Inverse Probl.*, *14*, 1–54, doi:10.1088/0266-5611/14/4/001.

Barbier, N., and P. Couteron (2015), Attenuating the bidirectional texture variation of satellite images of tropical forest canopies, *Remote Sens. Environ.*, *171*, 245–260, doi:10.1016/j.rse.2015.10.007.

Barbier, N., P. Couteron, C. Proisy, Y. Malhi, and J. P. Gastellu-Etchegorry (2010), The variation of apparent crown size and canopy heterogeneity across lowland Amazonian forests, *Global Ecol. Biogeogr.*, *19*(1), 72–84, doi:10.1111/j.1466-8238.2009.00493.x.

Bastin, A. J., N. Barbier, P. Couteron, B. Adams, A. Shapiro, J. Bogaert, and C. De Cannière (2014), Aboveground biomass mapping of African forest mosaics using canopy texture analysis: Toward a regional approach, *Ecol. Appl.*, *24*(8), 1984–2001.

Bastin, J.-F., et al. (2015), Seeing Central African forests through their largest trees, *Sci. Rep.*, *5*, 1–8, doi:10.1038/srep13156.

Bellassen, V., G. Le Maire, J. F. Dhôte, P. Ciais, and N. Viovy (2010), Modelling forest management within a global vegetation model—Part 1: Model structure and general behaviour, *Ecol. Model.*, *221*(20), 2458–2474, doi:10.1016/j.ecolmodel.2010.07.008.

Bellassen, V., G. le Maire, O. Guin, J. F. Dhôte, P. Ciais, and N. Viovy (2011), Modelling forest management within a global vegetation model-Part 2: Model validation from a tree to a continental scale, *Ecol. Modell.*, *222*(1), 57–75, doi:10.1016/j.ecolmodel.2010.08.038.

Blanchard, E., et al. (2016), Contrasted allometries between stem diameter, crown area, and tree height in five tropical biogeographic areas, *Trees-Struct. Funct.*, *30*(6), 1953–1968, doi:10.1007/s00468-016-1424-3.

van Bodegom, P. M., J. C. Douma, and L. M. Verheijen (2014), A fully traits-based approach to modeling global vegetation distribution, *Proc. Natl. Acad. Sci. U.S.A.*, *111*(38), 13733–8, doi:10.1073/pnas.1304551110.

Chave, J., D. Coomes, and S. Jansen (2009), Towards a worldwide wood economics spectrum, *Ecol. Lett.*, *351–366*, doi:10.1111/j.1461-0248.2009.01285.x.

Chave, J., et al. (2014), Improved allometric models to estimate the aboveground biomass of tropical trees, *Global Chang. Biol.*, *20*(10), 3177–3190, doi:10.1111/gcb.12629.

Ciais, P., et al. (2014), Current systematic carbon-cycle observations and the need for implementing a policy-relevant carbon observing system, *Biogeosciences*, *11*(13), 3547–3602, doi:10.5194/bg-11-3547-2014.

Couteron, P., R. Pelissier, E. A. Nicolini, and D. Paget (2005), Predicting tropical forest stand structure parameters from Fourier transform of very high-resolution remotely sensed canopy images, *J. Appl. Ecol.*, *42*(6), 1121–1128, doi:10.1111/j.1365-2664.2005.01097.x.

Deleuze, C., O. Pain, J. Dhote, and J.-C. Hervé (2004), A flexible radial increment model for individual trees in pure age stands, *Ann. For. Sci.*, *61*(4), 327–335, doi:10.1051/forest.

Dubois-Fernandez, P. C., T. Le Toan, S. Daniel, H. Oriot, J. Chave, L. Blanc, L. Villard, M. W. J. Davidson, and M. Petit (2012), The tropiSAR airborne campaign in French Guiana: Objectives, description, and observed temporal behavior of the backscatter signal, *IEEE Trans. Geosci. Remote Sens.*, *50*(8), 3228–3241, doi:10.1109/TGRS.2011.2180728.

Fauset, S., et al. (2015), Hyperdominance in Amazonian forest carbon cycling, *Nat. Commun.*, *6*, 6857, doi:10.1038/ncomms7857.

Goodman, R. C., O. L. Phillips, and T. R. Baker (2014), Ecological Archives A024-040-A1 Rosa C. Goodman, Oliver L. Phillips, and Timothy R. Baker. 2014. The importance of crown dimensions to improve tropical tree biomass estimates, *Ecol. Appl.*, *24*(4), 1–4.

Hansen, M. C., et al. (2013), High-resolution global maps of 21st-century forest cover change, *Science*, *342*(6160), 850–3, doi:10.1126/science.1244693.

Ho Tong Minh, D., T. Le Toan, F. Rocca, S. Tebaldini, M. M. D'Alessandro, and L. Villard (2014), Relating P-band synthetic aperture radar tomography to tropical forest biomass, *IEEE Trans. Geosci. Remote Sens.*, *52*(2), 967–979, doi:10.1109/TGRS.2013.2246170.

Tong Minh, D. H., et al. (2016), SAR tomography for the retrieval of forest biomass and height: Cross-validation at two tropical forest sites in French Guiana, *Remote Sens. Environ.*, *175*, 138–147, doi:10.1016/j.rse.2015.12.037.

Houghton, R. (2013), The emissions of carbon from deforestation and degradation in the tropics: Past trends and future potential, *Carbon Manag.*, *4*(5), 539–546, doi:10.4155/cmt.13.41.

Houghton, R. A., J. I. House, J. Pongratz, G. R. Van Der Werf, R. S. Defries, M. C. Hansen, C. Le Quéré, and N. Ramankutty (2012), Carbon emissions from land use and land-cover change, *Biogeosciences*, *9*(12), 5125–5142, doi:10.5194/bg-9-5125-2012.

Hurtt, G. C., R. Dubayah, J. Drake, P. R. Moorcroft, S. W. Pacala, J. B. Blair, and M. G. Fearon (2004), Beyond potential vegetation:Combining LIDAR data and a height-structured model for carbon studies, *Ecol. Appl.*, *14*(3), 873–883, doi:10.1890/02-5317.

Hurtt, G. C., J. Fisk, R. Q. Thomas, R. Dubayah, P. R. Moorcroft, and H. H. Shugart (2010), Linking models and data on vegetation structure, *J. Geophys. Res.*, *115*, G00E10, doi:10.1029/2009JG000937.

Kattge, J., et al. (2011), TRY—A global database of plant traits, *Global Chang. Biol.*, *17*(9), 2905–2935, doi:10.1111/j.1365-2486.2011.02451.x.

Kobayashi, K., and M. U. Salam (2000), Comparing simulated and measured values using mean squared desviation and its components, *Agron. J.*, *92*, 345–352, doi:10.1007/s100870050043.

Kohyama, T. (1992), Density-size dynamics of trees simulated by a one-sided competition multi-species model of rain forest stands, *Ann. Bot.*, *70*(5), 451–460, doi:10.1093/oxfordjournals.aob.a088502.

Krieger, G., A. Moreira, H. Fiedler, I. Hajnsek, M. Werner, M. Younis, and M. Zink (2007), TanDEM-X: A satellite formation for high-resolution SAR interferometry, *IEEE Trans. Geosci. Remote Sens.*, *45*(11), 3317–3340, doi:10.1109/TGRS.2007.900693.

Krinner, G., N. Viovy, N. de Noblet-Ducoudré, J. Ogée, J. Polcher, P. Friedlingstein, P. Ciais, S. Sitch, and I. C. Prentice (2005), A dynamic global vegetation model for studies of the coupled atmosphere-biosphere system, *Global Biogeochem. Cycles*, *19*, GB1015, doi:10.1029/2003GB002199.

Kugler, F., D. Schulze, I. Hajnsek, H. Pretzsch, and K.-P. Papathanassiou (2014), {TanDEM-X pol-InSAR} performance for Forest height estimation *EEE Trans. Geosci. Remote Sens.*, *52*(10), 6404–6422, doi:10.1109/TGRS.2013.2296533.

Lardy, R., G. Bellocchi, and J. F. Soussana (2011), A new method to determine soil organic carbon equilibrium, *Environ. Model. Softw.*, *26*(12), 1759–1763, doi:10.1016/j.envsoft.2011.05.016.

Lefsky, M. A. (2010), A global forest canopy height map from the moderate resolution imaging spectroradiometer and the geoscience laser altimeter system, *Geophys. Res. Lett.*, *37*, L15401, doi:10.1029/2010GL043622.

Mermoz, S., M. Réjou-Méchain, L. Villard, T. Le Toan, V. Rossi, and S. Gourlet-Fleury (2015), Decrease of L-band SAR backscatter with biomass of dense forests, *Remote Sens. Environ.*, *159*, 307–317, doi:10.1016/j.rse.2014.12.019.

Mitchard, E. (2015), Synthesis of the state of the art of aboveground biomass estimation using remote sensing, *high carbon Stock +*, (September).

Mitchard, E. T. A., et al. (2014), Markedly divergent estimates of Amazon forest carbon density from ground plots and satellites, *Glob. Ecol. Biogeogr.*, doi:10.1111/geb.12168.

Morton, D. C. (2016), Forest carbon fluxes: A satellite perspective, *Nat. Clim. Change*, *6*(4), 346–348, doi:10.1038/nclimate2978.

Naudts, K., et al. (2015), A vertically discretised canopy description for ORCHIDEE (SVN r2290) and the modifications to the energy, water and carbon fluxes, *Geosci. Model Dev.*, *8*(7), 2035–2065, doi:10.5194/gmd-8-2035-2015.

Phillips, O. L., et al. (2002), Changes in growth of tropical forests: Evaluating potential biases, *Ecol. Appl.*, *12*(2), 576–587.

Ploton, P., R. Pelissier, C. Proisy, T. Flavenot, N. Barbier, S. N. Rai, and P. Couteron (2012), Assessing aboveground tropical forest biomass using Google Earth canopy images, *Ecol. Appl.*, *22*(3), 993–1003, doi:10.1890/11-1606.1.

Ploton, P., R. Pelissier, N. Barbier, C. Proisy, B. R. Ramesh, and P. Couteron (2013), Canopy texture analysis for large-scale assessments of tropical forest stand structure and biomass, *Treetops Risk Challenges Glob. Canopy Ecol. Conserv.*, 1–444, doi:10.1007/978-1-4614-7161-5.

Proisy, C., P. Couteron, R. Pélissier, N. Barbier, and J. Engel (2007), Monitoring canopy grain of tropical forest using Fourier-based textural ordination (FOTO) of very high resolution images, *Int. Geosci. Remote Sens. Symp.*, 4324–4326, doi:10.1109/IGARSS.2007.4423808.

Pütz, S., J. Groeneveld, K. Henle, C. Knogge, A. C. Martensen, M. Metz, J. P. Metzger, M. C. Ribeiro, M. D. de Paula, and A. Huth (2014), Long-term carbon loss in fragmented Neotropical forests, *Nat. Commun.*, *5*, doi:10.1038/ncomms6037.

Le Quéré, C., et al. (2015), Global carbon budget 2015, *Earth Syst. Sci. Data*, *7*(2), 349–396, doi:10.5194/essd-7-349-2015.

Reineke, L. H. (1933), Perfecting a stand-density index for even-aged forests, *J. Agric. Res.*, *46*(7), 627–638.

Réjou-Méchain, M., B. Tymen, L. Blanc, S. Fauset, T. R. Feldpausch, A. Monteagudo, O. L. Phillips, H. Richard, and J. Chave (2015), Using repeated small-footprint LiDAR acquisitions to infer spatial and temporal variations of a high-biomass Neotropical forest, *Remote Sens. Environ.*, *169*(August), 93–101, doi:10.1016/j.rse.2015.08.001.

Richter, D., and R. Houghton (2011), Gross CO_2 fluxes from land-use change: Implications for reducing global emissions and increasing sinks, *Carbon Manag.*, *2*(1), 41–47, doi:10.4155/cmt.10.43.

Saatchi, S. S., et al. (2011), Benchmark map of forest carbon stocks in tropical regions across three continents, *Proc. Natl. Acad. Sci. U.S.A.*, *108*(24), 9899–904, doi:10.1073/pnas.1019576108.

Schlund, M., F. von Poncet, S. Kuntz, C. Schmullius, and D. H. Hoekman (2015), TanDEM-X data for aboveground biomass retrieval in a tropical peat swamp forest, *Remote Sens. Environ.*, *158*, 255–266, doi:10.1016/j.rse.2014.11.016.

Shimada, M., T. Tadono, and A. Rosenqvist (2010), Advanced land observing satellite (ALOS) and monitoring global environmental change, *Proc. IEEE*, *98*(5), 780–799, doi:10.1109/JPROC.2009.2033724.

Slik, J. W. F., et al. (2013), Large trees drive forest aboveground biomass variation in moist lowland forests across the tropics, *Glob. Ecol. Biogeogr.*, *22*(12), 1261–1271, doi:10.1111/geb.12092.

Stephenson, N. L. et al. (2014), Rate of tree carbon accumulation increases continuously with tree size., *Nature*, *507*(7490), 90–3, doi:10.1038/nature12914.

Stysley, P. R., D. B. Coyle, R. B. Kay, R. Frederickson, D. Poulios, K. Cory, and G. Clarke (2015), Long term performance of the High Output Maximum Efficiency Resonator (HOMER) laser for NASA's Global Ecosystem Dynamics Investigation (GEDI) lidar, *Opt. Laser Technol.*, *68*, 67–72, doi:10.1016/j.optlastec.2014.11.001.

Le Toan, T., S. Quegan, and M. Davidson (2011), The BIOMASS mission: Mapping global forest biomass to better understand the terrestrial carbon cycle, *Remote Sens. Environ.*, *115*, 2850–2860.

Vincent, G., D. Sabatier, L. Blanc, J. Chave, E. Weissenbacher, R. Pélissier, E. Fonty, J. F. Molino, and P. Couteron (2012), Accuracy of small footprint airborne LiDAR in its predictions of tropical moist forest stand structure, *Remote Sens. Environ.*, *125*, 23–33, doi:10.1016/j.rse.2012.06.019.

Wei, Y., et al. (2014), The north american carbon program multi-scale synthesis and terrestrial model intercomparison project—Part 2: Environmental driver data, *Geosci. Model Dev.*, *7*(6), 2875–2893, doi:10.5194/gmd-7-2875-2014.